Accepted Manuscript

An automated epifluorescence microscopy imaging assay for the identification of phospho-AKT level modulators in breast cancer cells

Elke Kaemmerer, Dane Turner, Amelia A. Peters, Sarah J. Roberts-Thomson, Gregory R. Monteith

PII: S1056-8719(17)30530-0
DOI: doi:10.1016/j.vascn.2018.02.005
Reference: JPM 6502

To appear in: *Journal of Pharmacological and Toxicological Methods*

Received date: 29 October 2017
Revised date: 28 January 2018
Accepted date: 8 February 2018

Please cite this article as: Elke Kaemmerer, Dane Turner, Amelia A. Peters, Sarah J. Roberts-Thomson, Gregory R. Monteith , An automated epifluorescence microscopy imaging assay for the identification of phospho-AKT level modulators in breast cancer cells. The address for the corresponding author was captured as affiliation for all authors. Please check if appropriate. Jpm(2018), doi:10.1016/j.vascn.2018.02.005

An automated epifluorescence microscopy imaging assay for the identification of phospho-AKT level modulators in breast cancer cells

Elke Kaemmerer[1,2,3,§], Dane Turner[1], Amelia A. Peters[1,2,3], Sarah J. Roberts-Thomson[1], Gregory R. Monteith[1,2,3]

[1]The School of Pharmacy, The University of Queensland, Brisbane, Queensland, Australia
[2]Mater Research Institute, The University of Queensland, Brisbane, Queensland, Australia
[3]Translational Research Institute, Brisbane, Queensland, Australia

To whom correspondence should be addressed: Prof Greg Monteith, School of Pharmacy, The University of Queensland, Pharmacy Australia Centre of Excellence, 20 Cornwall St, Woolloongabba 4072, Queensland, Australia. E-mail: gregm@uq.edu.au

[§]now Griffith University, Griffith Institute for Drug Discovery, Building N27 Don Young Road, Nathan, 4111, Queensland, Australia

Contact addresses of all authors

Elke Kaemmerer	e.kaemmerer@griffith.edu.au
Dane Turner	dane.turner@uqconnect.edu.au
Amelia A Peters	a.peters1@uq.edu.au
Sarah J. Roberts-Thomson	sarahrt@uq.edu.au
Greg R. Monteith	gregm@uq.edu.au

Abstract

AKT is an enzyme of the PI3K/pAKT pathway, regulating proliferation and cell survival. High basal levels of active, phosphorylated AKT (pAKT) are associated with tumor progression and therapeutic resistance in some breast cancer subtypes, including HER2 positive breast cancers. Various stimuli can increase pAKT levels and elevated basal pAKT levels are a feature of PTEN-deficient breast cancer cell lines. The aim of this study was to develop an assay able to identify modulators of pAKT levels using an automated epifluorescence microscope and high content analysis. To develop this assay, we used HCC-1569, a PTEN-deficient, HER2-overexpressing breast cancer cell line with elevated basal pAKT levels. HCC-1569 cells were treated with a selective pharmacological inhibitor of AKT (MK-2206) to reduce basal pAKT levels or EGF to increase pAKT levels. Immunofluorescence images were acquired using an automated epifluorescence microscope and integrated intensity of cytoplasmic pAKT staining was calculated using high content analysis software. Mean and median integrated cytoplasmic intensity were normalized using fold change and standard score to assess assay quality and to identify most robust data analysis. The highest z' factor was achieved for median data normalization using the standard score method (z' = 0.45). Using our developed assay we identified the calcium homeostasis regulating proteins TPRV6, STIM1 and TRPC1 as modulators of pAKT levels in HCC-1569 cells. Calcium signaling controls a diverse array of cellular processes and some calcium homeostasis regulating proteins are involved in modulating pAKT levels in cancer cells. Thus, these identified hits present promising targets for further assessment.

Keywords: assay development, automated microscopy, breast cancer, calcium channels, gene silencing, high content analysis

Abbreviations

EGF	Epidermal growth factor
EGFR	Epidermal growth factor receptor
EMT	Epithelial mesenchymal transition
HER2	Human epidermal growth factor receptor 2
pAKT	Phosphorylated AKT

PBS	Phosphate buffered saline
PBSCM	PBS containing calcium and magnesium
PI3K	Phosphatidylinositol-4,5-bisphosphate 3-kinase
PFA	Paraformaldehyde
PMCA	Plasma membrane Ca^{2+}- ATPase
PTEN	Phosphatase and tensin homolog
siNT	Non-targeting small interfering RNA
SPCA	Secretory pathway Ca^{2+}-ATPase
STIM	Stromal interaction molecule
TGF-β	Transforming growth factor β
TRPC	Transient receptor potential canonical
TRPV	Transient receptor potential vanilloid

Author contributions:

EK, DT performed all experiments and data analysis. GRM, SJRT designed the study and supervised experiments. AAP helped with study design and data analysis. All authors contributed to manuscript writing and read the final manuscript.

Disclosure statements

GM and SRT are associated with QUE Oncology.

Acknowledgement

This study was supported by the National Health and Medical Research Council (NHMRC, grant**:** 1079672) of Australia and The University of Queensland. GRM was supported by the Mater Foundation. The Translational Research Institute is supported by a grant from the Australian Government.

Introduction

Therapeutic responses and disease progression of breast cancers are highly dependent on the molecular/clinical subtype and the presence of druggable targets for hormonal or molecularly targeted therapy (Blows, et al., 2010). Progress in drug development, targeted therapies and early disease detection have improved overall survival for many breast cancer patients (Siegel, et al., 2012). However, intrinsic and acquired resistance to molecular targeted therapies are a major concern (Gonzalez-Angulo, Morales-Vasquez, & Hortobagyi, 2007). Hence, there is an urgent need to identify new therapeutic targets that are involved in modulating the activity of key enzymes in tumor-associated signaling pathways and therapeutic resistance (Luo, Manning, & Cantley, 2003).

A key pathway in regulating cell survival and proliferation is the PIP3/AKT pathway. Increased signaling through this pathway is found in many types of cancer and has been linked to drug resistance and thus targeting key enzymes of this pathway is of major interest. A main regulator of this pathway is AKT, a protein kinase, activated through phosphorylation of two residues (serine 473 and threonine 308), which can be initiated via diverse upstream mechanisms, e.g. epidermal growth factor (EGF) activation of the EGF receptor (EGFR) (Henson & Gibson, 2006; Luo, et al., 2003). AKT activity is enhanced in cancers with loss of function mutations or decreased expression of phosphatase and tensin homolog (PTEN), a negative AKT modulator (Nagata, et al., 2004). Some breast cancer cell lines, including HCC-1569, a human epidermal growth factor receptor 2 (HER2) overexpressing cell line of the basal molecular subtype, have a loss of PTEN and hence exhibit elevated levels of basal pAKT (Azimi, et al., 2017; deGraffenried, et al., 2004). Upregulated pAKT levels are linked to increased cell proliferation, reduced apoptosis and are involved in mediating resistance to HER2 targeted therapy and chemotherapy (Clark, West, Streicher, & Dennis, 2002; O'Brien, et al., 2010; Yang, et al., 2015). Targeting the PIP3/AKT pathway with pharmacological inhibitors represents a strategy to improve current treatment options and could potentially overcome resistance mechanisms in some breast cancer patients (ClinicalTrials.gov; Luo, et al., 2003; Yap, et al., 2011).

Traditionally immunoblotting or standard immunofluorescence imaging are used to assess pAKT levels. However, these methods only allow for low sample throughput and are not compatible with automation. One method to increase sample throughput is automated epifluorescence microscopy and high content analysis, which has been relatively unexplored to identify pAKT modulators in the published literature. High content analysis is a method using automated microscopy combined with multi-parameter imaging processing to produce

numerical data sets of detected imaging parameters for quantitative image analysis (Buchser, et al., 2004). Such an approach allows the fast assessment of pAKT levels in individual cells within a large cell population in each well at the same time.

Our study sought to develop such an assay to identify calcium homeostasis regulating proteins that modulate basal pAKT levels. Calcium signaling plays an important role in a diverse array of cellular processes relevant to tumor progression including proliferation, migration and apoptosis (Monteith, Davis, & Roberts-Thomson, 2012). Many breast cancers show altered expression of specific calcium channels and/or calcium pumps (Monteith, et al., 2012). Pharmacological inhibition or silencing of some of these calcium channels or pumps reduces breast cancer cell proliferation and/or invasiveness in *in vitro* and *in vivo* studies (Azimi, Roberts-Thomson, & Monteith, 2014). Recently the Ca^{2+} permeable ion channel TRPC1 was identified as a positive modulator of pAKT levels in PTEN-deficient breast cancer cell lines, whereby TRPC1 silencing decreases basal pAKT levels (Azimi, et al., 2017). The potential role of other calcium channels or even specific calcium pumps to regulate pAKT in PTEN-deficient breast cancer cells has not been fully explored. The pharmacological modulation of such calcium channels and pumps may provide an opportunity to reduce AKT activation in breast cancer cells without the possible systemic side effects of global AKT inhibition. Such agents could be used in combination with or instead of direct AKT inhibitors, e.g. MK-2206, used in a clinical trial for advanced breast cancers to improve treatment outcome (ClinicalTrials.gov). This paper is specifically for academic laboratories who are considering or planning to use an automated epi-fluorescence microscopy approach for targeted smaller scale screens for pAKT effects, the methodological considerations and validation approaches are described and discussed

Material and methods

Cell culture

HCC-1569 cells were maintained in RPMI-1640 media (Sigma Aldrich, R8757) supplemented with 10 % fetal bovine serum (FBS) (complete growth media), at 37 °C with 5 % CO_2. Cells were routinely tested for mycoplasma contamination (MycoAlert, Lonza, Basel, Switzerland) and authenticated by STR profiling (GenePrint 10 system; Promega, Madison, WA, USA) at QIMR Berghofer, Brisbane, Australia.

siRNA transfection

Cells were seeded into 96-well black-walled clear bottom imaging plates (353219, BD Biosciences) at a density of 5000 cells/well and transfected with siRNA 24 h after seeding. For siRNA experiments cells were treated with Dharmacon ON-TARGET*plus* SMARTpool siRNA (GE Dharmacon, Lafayette, CO, USA) at a final concentration of 100 nM/well and DharmaFECT4 transfection reagent (0.1 µL/well, Dharmacon, T-2004-01) in media containing 8 % FBS, according to the company's recommended protocol. The following Dharmacon ON-TARGET*plus* SMARTpool siRNAs were used in this study: Non-targeting (D-001810-10-05), TRPC1 (L-004191-00-0005), TRPV6 (L-003607-00-0005), STIM1 (L-011785-00-0005), ORAI1 (L-014998-00-0005), PMCA1 (L-006115-00-0005), PMCA2 (L-006116-00-0005), PMCA4 (L-006118-00-0005), SPCA1 (L-006119-00-0005) and SPCA2 (L-006280-00-0005). These targets were assessed due to their potential contribution to basal and/or trans-golgi network Ca^{2+} levels.

Induction and inhibition of AKT phosphorylation using EGF and MK-2206

Forty-eight hours post siRNA transfection cell culture medium was serum reduced (0.5 % FBS) for 24 h before cells were treated with 1 µM of AKT Inhibitor MK-2206 2HCl (Selleckchem, 1032350) or 0.1 % DMSO (vehicle control) in serum reduced media. AKT phosphorylation was induced 24 h after inhibitor treatement with EGF (60 ng/mL; Sigma-Aldrich, E9644) or vehicle control (0.5 µM acetic acid) in serum reduced media for 20-25 min. Cells were then fixed and stained as described below.

Immunofluorescence

Plates were chilled on ice and cells were washed twice with Phosphate Buffered Saline (PBS) containing 0.1 mM $CaCl_2$, 1 mM $MgCl_2$ (PBSCM). Cells were fixed with 4 % PFA (Pierce, Thermo Fischer Scientific, 28906) in PBSCM for 20 min, washed once in PBSCM/0.1 M Glycine, twice in PBS/CM and then permeabilized with 0.2 % (v/v) Triton-X-

100/PBSCM for 10 min before washed 3 times in PBSCM. Cells were then incubated in blocking buffer (PBSCM and 1 % BSA) for 1 h at room temperature before incubation with primary antibody (pAKT (Ser473), 4060 Cell Signaling) at a 1:100 dilution in blocking buffer (PBSCM and 1 % BSA) overnight at 4 °C. Cells were washed 3 times in PBSCM before incubation with secondary antibody in blocking buffer (anti-Rabbit IgG, Alexa Fluor® 488 Conjugate, 4412 Cell Signaling) at a 1:1000 dilution for 1 h at room temperature. Cells were washed twice before nuclei were stained using 2 µg/mL DAPI in PBSCM for 10 min and washed twice in PBSCM before cells were imaged in PBS. All steps were performed using an electronic multichannel pipette at low speed to minimize cell loss during this staining protocol.

Image acquisition and analysis

Cells were imaged using an ImageXpress Micro automated epifluorescence microscope (Molecular Devices, Sunnyvale CA, USA) with a 10x objective and the following excitation/emission filters: wavelength 377–450 nm/447-60 nm for DAPI (W1: DAPI filter) and 472-530 nm/520-630 nm for Alexa488 (W2: GFP filter). Images of duplicate wells in each plate were acquired with 100 ms (DAPI filter, nuclei) and 4357 ms (GFP filter, pAKT) exposure times. Seven sites per well were imaged (sites were separate from each other to avoid photo bleaching). Laser based autofocusing was used for each site. For single cell analysis images were acquired and analyzed using the MetaXpress software. Cells were identified for nuclear count using the following parameters, nuclei staining with a minimum of 10 and maximum of 40 µm widths (16-62 pixels) and an intensity of 1000 graylevels above local background. For pAKT staining, cells were identified with a cytoplasm staining with a minimum of 15 µm and a maximum of 80 µm widths (23-124 pixels) and an intensity of 80 graylevels above local background.

Immunoblotting

Protein was isolated from eight pooled wells of a 96-well plate using protein lysis buffer supplemented with protease and phosphatase inhibitors (Roche Applied Science, Penzberg, Germany). Gel electrophoresis was performed using mini protean TGX stain free precast gels (Bio-Rad, Gladesville, New South Wales) with 1x TGX running buffer (Bio-Rad) and transferred to a PVDF membrane (Bio-Rad) using the Trans Blot Turbo Transfer system (Bio-Rad). Membranes were blocked in 0.1 % PBST + 5 % skim milk for 1 h. Primary pAKT antibody (Phospho-Akt (Ser473), 4051, Cell Signaling) and AKT antibody (Akt Antibody, 9272, Cell Signaling) were diluted 1:1000 in blocking buffer and incubated at 4 °C overnight. The following secondary antibodies were used; anti-mouse HRP-conjugated secondary

(170–6516, Bio-Rad) and anti-rabbit HRP-conjugated secondary (170–6515 BioRad) at 1:10 000 dilution. Images were acquired using the Chemidoc Touch Imaging System (Bio-Rad), analyzed using the ImageLab software version 5.2.1 (Bio-Rad) and local background subtraction. Protein density was normalized to beta actin loading controls and pAKT protein expression was normalized to total AKT protein expression as previously described (Azimi, et al., 2017).

Data analysis and statistics

Single cell data from seven fields/well were analyzed using MetaXpress and exported to Excel, zero values were not further analyzed. All data was log transformed and statistical analysis was performed using GraphPad Prism. Tests used for statistical significance are found in each figure legend.

Formulas

Standard score

$$SS = \frac{X_{cell} - \mu_{plate}}{\sigma_{plate}}$$

X = log cytoplasmic intensity of pAKT staining of a single identified cell

μ_{plate} = mean of log cytoplasmic intensity of pAKT staining of all identified cells per plate, for all treatments (control, EGF and MK-2206 treated cells in duplicate wells per plate)

σ_{plate} = standard deviation of log cytoplasmic intensity of pAKT staining of all identified cells per plate (control, EGF and MK-2206 treated cells in duplicate wells per plate)

z' factor

$$z' = 1 - \frac{3(\sigma_{pos} + \sigma_{neg})}{|\mu_{pos} - \mu_{neg}|}$$

σ_{pos} = standard deviation of log cytoplasmic intensity of pAKT staining of all identified cells in positive control wells (EGF treated cells) of all 3 experiments

σ_{pos} = standard deviation of log cytoplasmic intensity of pAKT staining of all identified cells in negative control wells (MK-2206 treated cells) of all 3 experiments

μ_{pos} = mean of log cytoplasmic intensity of pAKT staining of all identified cells in positive control wells (EGF treated cells) of all 3 experiments

μ_{neg} = mean of log cytoplasmic intensity of pAKT staining of all identified cells in negative control wells (MK-2206 treated cells) of all 3 experiments

Results

In this study, we present an assay with increased throughput suitable to identify potential modulators of AKT phosphorylation using immunofluorescence imaging with an automated epifluorescence microscope and high content analysis. This assay was optimized using the PTEN deficient breast cancer cell line (HCC-1569), which exhibits high basal levels of pAKT, and positive and negative controls, EGF (induces AKT phosphorylation, positive control) (Henson & Gibson, 2006) and the pharmacological AKT inhibitor MK-2206 (reduces AKT phosphorylation negative control) (Hirai, et al., 2010).

The first step to establish our assay protocol was to assess pAKT levels in HCC-1569 cells after treatment with a known negative and a known positive pAKT modulator using immunofluorescence imaging. We then compared the log integrated cytoplasmic staining intensity for pAKT. HCC-1569 cells were treated with vehicle control (Fig. $1A_i$), a pharmacological AKT Inhibitor (MK-2206) (Fig. $1A_{ii}$) or stimulated with EGF (Fig $1A_{iii}$) and imaged using an automated epifluorescence microscope. As expected, basal AKT phosphorylation levels appeared to increase with EGF and decrease with MK-2206 treatment. This data was then analyzed using high content imaging analysis, with an inbuilt algorithm for nuclear cell count (MetaXpress) to identify cells and to assess their log integrated cytoplasmic intensity for pAKT staining (Fig. 1B). Treatment with MK-2206 resulted in a significant reduction of the integrated log cytoplasmic intensity compared to vehicle controls, whereas EGF treatment significantly increased the pAKT level (Fig. 1B).

Although significant, the mean of the raw data values of the integrated log cytoplasmic intensity between treatments was very similar and thus the assay window very small. To be able to compare raw data sets of log cytoplasmic intensity values and to improve the assay window, different normalization methods were applied (Fig 2). To identify the most robust normalization approach and optimal analysis method for this assay, the z' factor was calculated for each method. The z' factor is a statistically measurement widely used in high throughput screening to determine the robustness of an assay and to determine intra-plate variability (Zhang, Chung, & Oldenburg, 1999), a z' factor < 0 indicating a poor assay quality, a z' factor between 0 to 0.5 is considered suitable for medium throughput screening, while a score between 0.5 to 1 is indicative of an assay suitable for high throughput screening. We sought to use the z' factor to assess the effect of different normalization methods on the quality of this assay, by comparing normalized data sets from 3 different experiments. The log integrated cytoplasmic intensity was analyzed in duplicate wells per treatment (Fig 2A). A high inter-plate variability was observed, whereas technical replicates on each plate showed

high reproducibility (Fig. 2A), resulting in a poor z' factor for a biomolecular screen (z' = -2.64). The mean of each replicate was normalized to the mean of the two control wells of the same plate to calculate the fold change (Fig. 2B), and this improved assay robustness (z' = 0). The standard score of the mean represents a potentially more robust way to normalize data, and this resulted in a z' factor of 0.37 (Fig. 2C). In addition to the mean, we compared different percentiles of the cytoplasmic intensity between the treatments. Leading us to adopt the standard score of the median, which had the highest z' factor and provided the largest assay window (z' = 0.45) (Fig. 2D).

Some calcium transporting proteins are involved in mediating drug resistance and are involved in pAKT regulation. Thus, we sought to examine the effect of gene silencing of nine different calcium homeostasis regulating proteins on pAKT levels in HCC-1569 breast cancer cells using our image based assay and optimized data normalization method (Fig 3). Gene silencing experiments were performed over 7 days (Fig 3A) and images were processed using high content imaging analysis (Fig 3B). As expected the positive control, EGF treatment, increased the median standard score and the negative control, MK-2206 treatment, reduced the standard score compared to siNT controls. Values higher than the mean of the median standard score for siNT controls were categorized as positive pAKT potential modulators (Fig 3C, above dotted line) and values lower as negative pAKT potential modulators (Fig 3C, below dotted line). Silencing of PMCA1, PMCA2 and PMCA4 did not affect the pAKT level, as values were similar to the control (siNT). In contrast, the silencing of SPCA1 and SPCA2 resulted in an increase of the median standard score, similar to EGF treated samples (Fig 3C). As we aimed to identify targets that when silenced reduced basal pAKT levels in HCC-1569 breast cancer cells, these targets were not further investigated.

Silencing of TRPV6, ORAI1, STIM1 and TRPC1 reduced pAKT level. The greatest reduction in pAKT levels was observed when TRPC1 was silenced, with a median standard score for the integrated log cytoplasmic intensity, similar to cells treated with MK-2206 (Fig 3C). TRPV6 silencing showed the second lowest standard score in this assay. Silencing of STIM1 reduced the median standard score only slightly and values were just lower than the lowest value of the control. Although ORAI1 silencing resulted in a reduction of the median standard score compared to the siNT control, these values were within the standard deviation of the controls. Thus, ORAI1 was not further investigated.

To confirm hits identified with our imaging based assay, an alternative low throughput method (immunoblotting) was used. Three targets, TRPC1, TRPV6 and STIM1, identified in

this screen as showing high, moderate and weak reduction of log cytoplasmic intensity compared to controls respectively, were validated using immunoblotting and a different primary antibody (optimized for immunoblotting) (Fig. 4A).

These three targets were silenced and experiments were performed following the described timeline with protein isolation for immunoblotting on day 6 instead of sample processing for immunofluorescence (Fig 3A). Immunoblotting results confirmed that silencing of all three targets reduced pAKT levels. Silencing of TRPV6 showed a 34 % reduction of pAKT levels compared to controls while silencing of STIM1 reduced pAKT levels by 56 %. Consistent with the automated immunofluorescence assay TRPC1 had the most pronounced effect on pAKT levels with a reduction of 71 % (Fig 4B). This immunoblotting assay confirmed the results of the high content imaging approach, suggesting the suitability of this image-based assay to identify new modulators of pAKT in PTEN deficient breast cancer cells.

Discussion

AKT phosphorylation is an important cellular regulatory switch of various downstream signaling pathways, many of which are relevant to cancer progression (Luo, et al., 2003; Yang, et al., 2015). Elevated levels of pAKT are found in breast cancers with loss of PTEN, as well as breast cancers with BRCA1 mutations or HER2 overexpression (Clark, et al., 2002; Vara, et al., 2004; Yi, et al., 2013). The PIP3/AKT pathway is involved in suppressing apoptosis, stimulating cell cycle progression and contributes to resistance to radiation and targeted therapy (Albert, Kim, Cao, & Lu, 2006; O'Brien, et al., 2010). Targeting AKT phosphorylation might present a new therapeutic approach to improve current management of advanced breast cancers (Hirai, et al., 2010; Luo, et al., 2003). This study presents a simple protocol to identify pAKT modulators using an automated epifluorescence imaging system and high content imaging analysis, rather than immunoblotting to quantify and compare AKT phosphorylation (Lin, Hsieh, Song, & Lin, 2005). Our assay protocol increases throughput and has been proven to be suitable to detect pAKT modulators. We showed that our automated epifluorescence microscopy based assay can identify modulators of AKT phosphorylation with medium throughput. During development of this assay, we consistently showed a signal increase in log cytoplasmic intensity for pAKT staining in HCC-1569 cells treated with the positive modulator (EGF) and a decrease for cells treated with the negative modulator (MK-2206) compared to pAKT levels in controls. However, we observed a high inter-plate variability, thus we sought to explore different normalization methods. A widely used method to normalize treated samples to controls is the fold change or ‘fraction of control’. Our data set was analyzed using this method normalizing the mean of each treatment (siNT + EGF, siNT + MK-2206) to the siNT control. However, this normalization method does not account for inter-plate variation of the log integrated cytoplasmic intensity. Thus, we used the standard score to normalize the data sets. The standard score converts the log integrated cytoplasmic intensity for pAKT staining for each individual cell into the number of standard deviations it differs from the plate mean, which resulted in a higher z’ factor (Malo, Hanley, Cerquozzi, Pelletier, & Nadon, 2006). Once the standard score was determined to be a suitable method for data normalization, the assay was further optimized by comparing different statistical measurements. The median standard score value resulted in the highest z’ factor.

As part of validating the new assay, we also assessed the effect of various calcium homeostasis regulating proteins on AKT phosphorylation in HCC-1569 breast cancer cells. Altered expression of calcium homeostasis regulating proteins has been associated with drug resistance in some breast cancer cells. For example, the transient receptor potential

channel TRPC5 promotes adriamycin resistance in MCF-7/ADM breast cancer cells (Ma, et al., 2012). Another study showed that silencing the calcium pump plasma membrane Ca^{2+}-ATPase 2 (PMCA2) in MDA-MB-231 basal breast cancer cells increased the efficacy of the chemotherapeutic doxorubicin (Peters, et al., 2016). TRPC1 and STIM1 have been linked to transforming growth factor β (TGFβ)-induced epithelial-to-mesenchymal transition (EMT) and to cancer metastasis in breast cancer (Schaar, Sukumaran, Sun, Dhasarathy, & Singh, 2016). A recent study showed that TRPC1 is a key regulator of a variety of hypoxia mediated changes and AKT signaling in PTEN deficient MDA-MB-468, TRPC1 was also shown to regulate AKT phosphorylation in HCC-1569 breast cancer cells (Azimi, et al., 2017). The mechanism by which TRPC1 contributes to pAKT and proliferation in breast cancer is likely multifactorial, but there is strong evidence for the involvement of TRPC1 in the regulation of basal Ca^{2+} influx in another PTEN deficient breast cancer cell line, MDA-MB-468 (Davis, et al., 2012). The finding that STIM1 reduced pAKT levels is of interest given the reports of STIM1 regulation of TRPC1-mediated effects in some cells (Huang, et al., 2006; Ng, et al., 2009; Schaar, et al., 2016). AKT phosphorylation may be dependent on basal calcim influx since TRPV6 silencing significantly reduced pAKT levels in HCC-1569 cells and TRPV6 is a constitutively active Ca^{2+} channel and a key regulator of basal Ca^{2+} influx (Peters, et al., 2012; Raphaël & Prevarskaya, 2012).

High content analysis allows the simultaneous assessment of a variety of phenotypic characteristics using a high throughput approach (Buchser, et al., 2004). Our assay was optimized for increased throughput to assess potential pAKT modulators, using a simple protocol, with inbuilt algorithms for assessment of cytosolic pAKT and the standard score normalization method. This assay facilitated the assessment of the effect of silencing proteins involved in calcium signaling on AKT phosphorylation and has the potential to identify other modulators of AKT phosphorylation. The molecular AKT modulators identified here (TRPC1, STIM1 and TRPV6) should now be further assessed using downstream assays to further define their roles in the pAKT/PIP3 pathway.

Fig 1: Induction and inhibition of AKT phosphorylation in HCC-1569 cells. pAKT levels in HCC-1569 cells transfected with siNT (vehicle control, Ai), treated with the AKT inhibitor MK-2206 for 24 h (A_{ii}), or 60 ng/mL EGF for 20-25 min (A_{iii}). Images were acquired using an automated epifluorescence microscope (ImageXpress, Molecular Devices) a DAPI filter set (Ex 377-450 nm/Em 447-560 nm) and a GFP filter set (Ex 472-530 nm/Em 520-535 nm). Images show nuclei in blue (DAPI staining, left panel), pAKT staining in green (Alexa Fluor® 488 Conjugate, mid panel) and the composite image of both images (right panel) (A). pAKT levels were analyzed in cells meeting criteria for signal intensity and stained area for both channels described in material and methods. Cytoplasmic intensity of the green channel (pAKT) was determined for controls, cells treated with the AKT inhibitor MK-2206 or EGF (n = 3 independent biological repeats, with 2 technical replicates ± SD, shown are 3000 randomized data points per treatment) (B). Statistical analysis was performed after log transformation compared to siNT using a one-way ANOVA with Dunnett's multiple comparison post-hoc analysis (*p* ****< 0.0001).

Fig 2: Assessment of log integrated cytoplasmic intensity of pAKT levels in HCC-1569 cells using different normalization methods. Values for log integrated cytoplasmic intensity, and z' factors are shown for mean (A), fold change (B), standard score of mean log integrated cytoplasmic intensity (C) and standard score of median log integrated cytoplasmic intensity (D) for HCC-1569 cells treated with siNT, siNT +EGF and siNT+ MK-2206 (n = 3 independent biological repeats, with 2 technical replicates ± SD).

Fig 3: Effect of silencing calcium homeostasis regulating proteins on pAKT levels in HCC-1569 breast cancer cells. Timeline for cell treatment (A). For image analysis, the multi wavelength scoring tool with a standard algorithm based on scoring for nuclei using wavelength 1, (W1: DAPI filter, B top panel) and cytoplasmic staining for pAKT using wavelength 2 (W2: GFP filter, B bottom panel) were applied. Identified objects for W1 are shown in white and for W2 in red (B). Calcium homeostasis regulating proteins were silenced and the standard score for median log cytoplasmic integrated intensity was compared to the mean of median standard score for the siNT controls (C). Values for the negative control (MK-2206) and the positive control (EGF) are also shown. Positive pAKT modulators were identified with values higher than the median standard score for siNT (above the dotted line) and negative pAKT modulators with lower values, non-targeting siRNA (siNT), TRPC1 siRNA (siTRPC1), TRPV6 siRNA (siTRPV6), ORAI1 siRNA (siORAI1), STIM1 siRNA (siSTIM1), SPCA1 siRNA (siSPCA1), SPCA2 siRNA (siSPCA2), PMCA1 siRNA (siPMCA1), PMCA2 siRNA (siPMCA2) or PMCA4 siRNA (siPMCA4) (siNT, siNT + EGF, siNT + MK-2206, n = 3 biological replicates, with 2 technical replicates;

silencing calcium homeostasis regulating proteins n = 1 biological replicate, 2 technical replicates).

Fig 4: Confirmation of identified negative pAKT modulators, TRPC1, STIM1 and TRPV6 using immunoblotting. Cells were treated with non-targeting siRNA (siNT), TRPV6 siRNA (siTRPV6), STIM1 siRNA (siSTIM1) or TRPC1 siRNA (siTRPC1). Representative immunoblots for pAKT, total AKT and their corresponding loading controls are shown in (A). pAKT and total AKT protein expression were normalized to the beta actin loading control and pAKT levels were expressed as relative to total AKT level (B). All bar graphs are mean ± SD (n = 3 biological replicates). Statistical analysis was performed using one-way ANOVA with Dunnett's multiple comparison post-hoc analysis comparing all treatments to siNT control (*p ≤ 0.05, p** ≤ 0.01, p*** ≤ 0.001).

References:

Albert, J. M., Kim, K. W., Cao, C., & Lu, B. (2006). Targeting the Akt/mammalian target of rapamycin pathway for radiosensitization of breast cancer. *Mol Cancer Ther, 5*, 1183-1189.

Azimi, I., Milevskiy, M. J. G., Kaemmerer, E., Turner, D., Yapa, K. T. D. S., Brown, M. A., Thompson, E. W., Roberts-Thomson, S. J., & Monteith, G. R. (2017). TRPC1 is a differential regulator of hypoxia-mediated events and Akt signalling in PTEN-deficient breast cancer cells. *Journal of Cell Science, 130*, 2292-2305.

Azimi, I., Roberts-Thomson, S. J., & Monteith, G. R. (2014). Calcium influx pathways in breast cancer: opportunities for pharmacological intervention. *British Journal of Pharmacology, 171*, 945-960.

Blows, F. M., Driver, K. E., Schmidt, M. K., Broeks, A., van Leeuwen, F. E., Wesseling, J., Cheang, M. C., Gelmon, K., Nielsen, T. O., Blomqvist, C., Heikkilä, P., Heikkinen, T., Nevanlinna, H., Akslen, L. A., Bégin, L. R., Foulkes, W. D., Couch, F. J., Wang, X., Cafourek, V., Olson, J. E., Baglietto, L., Giles, G. G., Severi, G., McLean, C. A., Southey, M. C., Rakha, E., Green, A. R., Ellis, I. O., Sherman, M. E., Lissowska, J., Anderson, W. F., Cox, A., Cross, S. S., Reed, M. W. R., Provenzano, E., Dawson, S.-J., Dunning, A. M., Humphreys, M., Easton, D. F., García-Closas, M., Caldas, C., Pharoah, P. D., & Huntsman, D. (2010). Subtyping of Breast Cancer by Immunohistochemistry to Investigate a Relationship between Subtype and Short and Long Term Survival: A Collaborative Analysis of Data for 10,159 Cases from 12 Studies. *PLOS Medicine, 7*, e1000279.

Buchser, W., Collins, M., Garyantes, T., Guha, R., Haney, S., Lemmon, V., Li, Z., & Trask, O. J. (2004). Assay Development Guidelines for Image-Based High Content Screening, High Content Analysis and High Content Imaging. In G. S. Sittampalam, N. P. Coussens, K. Brimacombe, A. Grossman, M. Arkin, D. Auld, C. Austin, J. Baell, B. Bejcek, T. D. Y. Chung, J. L. Dahlin, V. Devanaryan, T. L. Foley, M. Glicksman, M. D. Hall, J. V. Hass, J. Inglese, P. W. Iversen, S. D. Kahl, S. C. Kales, M. Lal-Nag, Z. Li, J. McGee, O. McManus, T. Riss, O. J. Trask, Jr., J. R. Weidner, M. Xia & X. Xu (Eds.), *Assay Guidance Manual*. Bethesda (MD).

Clark, A. S., West, K., Streicher, S., & Dennis, P. A. (2002). Constitutive and Inducible Akt Activity Promotes Resistance to Chemotherapy, Trastuzumab, or Tamoxifen in Breast Cancer Cells. *Molecular Cancer Therapeutics, 1*, 707-717.

ClinicalTrials.gov. https://clinicaltrials.gov/show/NCT01277757. In (Vol. 2017).

Davis, F. M., Peters, A. A., Grice, D. M., Cabot, P. J., Parat, M.-O., Roberts-Thomson, S. J., & Monteith, G. R. (2012). Non-Stimulated, Agonist-Stimulated and Store-Operated Ca2+ Influx in MDA-MB-468 Breast Cancer Cells and the Effect of EGF-Induced EMT on Calcium Entry. *PLOS ONE, 7*, e36923.

deGraffenried, L. A., Fulcher, L., Friedrichs, W. E., Grünwald, V., Ray, R. B., & Hidalgo, M. (2004). Reduced PTEN expression in breast cancer cells confers susceptibility to inhibitors of the PI3 kinase/Akt pathway. *Annals of Oncology, 15*, 1510-1516.

Gonzalez-Angulo, A. M., Morales-Vasquez, F., & Hortobagyi, G. N. (2007). Overview of resistance to systemic therapy in patients with breast cancer. *Adv Exp Med Biol, 608*, 1-22.

Henson, E. S., & Gibson, S. B. (2006). Surviving cell death through epidermal growth factor (EGF) signal transduction pathways: Implications for cancer therapy. *Cellular Signalling, 18*, 2089-2097.

Hirai, H., Sootome, H., Nakatsuru, Y., Miyama, K., Taguchi, S., Tsujioka, K., Ueno, Y., Hatch, H., Majumder, P. K., Pan, B.-S., & Kotani, H. (2010). MK-2206, an Allosteric Akt Inhibitor, Enhances Antitumor Efficacy by Standard Chemotherapeutic Agents or Molecular Targeted Drugs In vitro and In vivo. *Molecular Cancer Therapeutics, 9*, 1956-1967.

Huang, G. N., Zeng, W., Kim, J. Y., Yuan, J. P., Han, L., Muallem, S., & Worley, P. F. (2006). STIM1 carboxyl-terminus activates native SOC, Icrac and TRPC1 channels. *Nat Cell Biol, 8*, 1003-1010.

Lin, H. J., Hsieh, F. C., Song, H., & Lin, J. (2005). Elevated phosphorylation and activation of PDK-1//AKT pathway in human breast cancer. *Br J Cancer, 93*, 1372-1381.

Luo, J., Manning, B. D., & Cantley, L. C. (2003). Targeting the PI3K-Akt pathway in human cancer. *Cancer Cell, 4*, 257-262.

Ma, X., Cai, Y., He, D., Zou, C., Zhang, P., Lo, C. Y., Xu, Z., Chan, F. L., Yu, S., & Chen, Y. (2012). Transient receptor potential channel TRPC5 is essential for P-glycoprotein induction in drug-resistant cancer cells. *Proceedings of the National Academy of Sciences, 109*, 16282-16287.

Malo, N., Hanley, J. A., Cerquozzi, S., Pelletier, J., & Nadon, R. (2006). Statistical practice in high-throughput screening data analysis. *Nature biotechnology, 24*, 167.

Monteith, G. R., Davis, F. M., & Roberts-Thomson, S. J. (2012). Calcium channels and pumps in cancer: changes and consequences. *Journal of Biological Chemistry, 287*, 31666-31673.

Nagata, Y., Lan, K.-H., Zhou, X., Tan, M., Esteva, F. J., Sahin, A. A., Klos, K. S., Li, P., Monia, B. P., & Nguyen, N. T. (2004). PTEN activation contributes to tumor inhibition by trastuzumab, and loss of PTEN predicts trastuzumab resistance in patients. *Cancer Cell, 6*, 117-127.

Ng, L. C., McCormack, M. D., Airey, J. A., Singer, C. A., Keller, P. S., Shen, X. M., & Hume, J. R. (2009). TRPC1 and STIM1 mediate capacitative Ca2+ entry in mouse pulmonary arterial smooth muscle cells. *The Journal of physiology, 587*, 2429-2442.

O'Brien, N. A., Browne, B. C., Chow, L., Wang, Y., Ginther, C., Arboleda, J., Duffy, M. J., Crown, J., O'Donovan, N., & Slamon, D. J. (2010). Activated phosphoinositide 3-kinase/AKT signaling confers resistance to trastuzumab but not lapatinib. *Molecular Cancer Therapeutics, 9*, 1489-1502.

Peters, A. A., Milevskiy, M. J., Lee, W. C., Curry, M. C., Smart, C. E., Saunus, J. M., Reid, L., Da Silva, L., Marcial, D. L., & Dray, E. (2016). The calcium pump plasma membrane Ca2+-ATPase 2 (PMCA2) regulates breast cancer cell proliferation and sensitivity to doxorubicin. *Scientific reports, 6*, 25505.

Peters, A. A., Simpson, P. T., Bassett, J. J., Lee, J. M., Da Silva, L., Reid, L. E., Song, S., Parat, M.-O., Lakhani, S. R., & Kenny, P. A. (2012). Calcium Channel TRPV6 as a Potential Therapeutic Target in Estrogen Receptor–Negative Breast Cancer. *Molecular Cancer Therapeutics, 11*, 2158-2168.

Raphaël, M., & Prevarskaya, N. (2012). The role of the TRPV6 channel in cancer. *The Journal of physiology, 590*, 1369-1376.

Schaar, A., Sukumaran, P., Sun, Y., Dhasarathy, A., & Singh, B. B. (2016). TRPC1-STIM1 activation modulates transforming growth factor β-induced epithelial-to-mesenchymal transition. *Oncotarget, 7*, 80554.

Siegel, R., DeSantis, C., Virgo, K., Stein, K., Mariotto, A., Smith, T., Cooper, D., Gansler, T., Lerro, C., & Fedewa, S. (2012). Cancer treatment and survivorship statistics, 2012. *CA: a cancer journal for clinicians, 62*, 220-241.

Vara, J. Á. F., Casado, E., de Castro, J., Cejas, P., Belda-Iniesta, C., & González-Barón, M. (2004). PI3K/Akt signalling pathway and cancer. *Cancer treatment reviews, 30*, 193-204.

Yang, Z.-Y., Di, M.-Y., Yuan, J.-Q., Shen, W.-X., Zheng, D.-Y., Chen, J.-Z., Mao, C., & Tang, J.-L. (2015). The prognostic value of phosphorylated Akt in breast cancer: a systematic review. *Scientific reports, 5*, 7758.

Yap, T. A., Yan, L., Patnaik, A., Fearen, I., Olmos, D., Papadopoulos, K., Baird, R. D., Delgado, L., Taylor, A., & Lupinacci, L. (2011). First-in-man clinical trial of the oral pan-AKT inhibitor MK-2206 in patients with advanced solid tumors. *Journal of clinical oncology, 29*, 4688-4695.

Yi, Y. W., Kang, H. J., Kim, H. J., Hwang, J. S., Wang, A., & Bae, I. (2013). Inhibition of constitutively activated phosphoinositide 3-kinase/AKT pathway enhances antitumor activity of chemotherapeutic agents in breast cancer susceptibility gene 1-defective breast cancer cells. *Molecular carcinogenesis, 52*, 667-675.

Zhang, J.-H., Chung, T. D. Y., & Oldenburg, K. R. (1999). A Simple Statistical Parameter for Use in Evaluation and Validation of High Throughput Screening Assays. *Journal of Biomolecular Screening, 4*, 67-73.

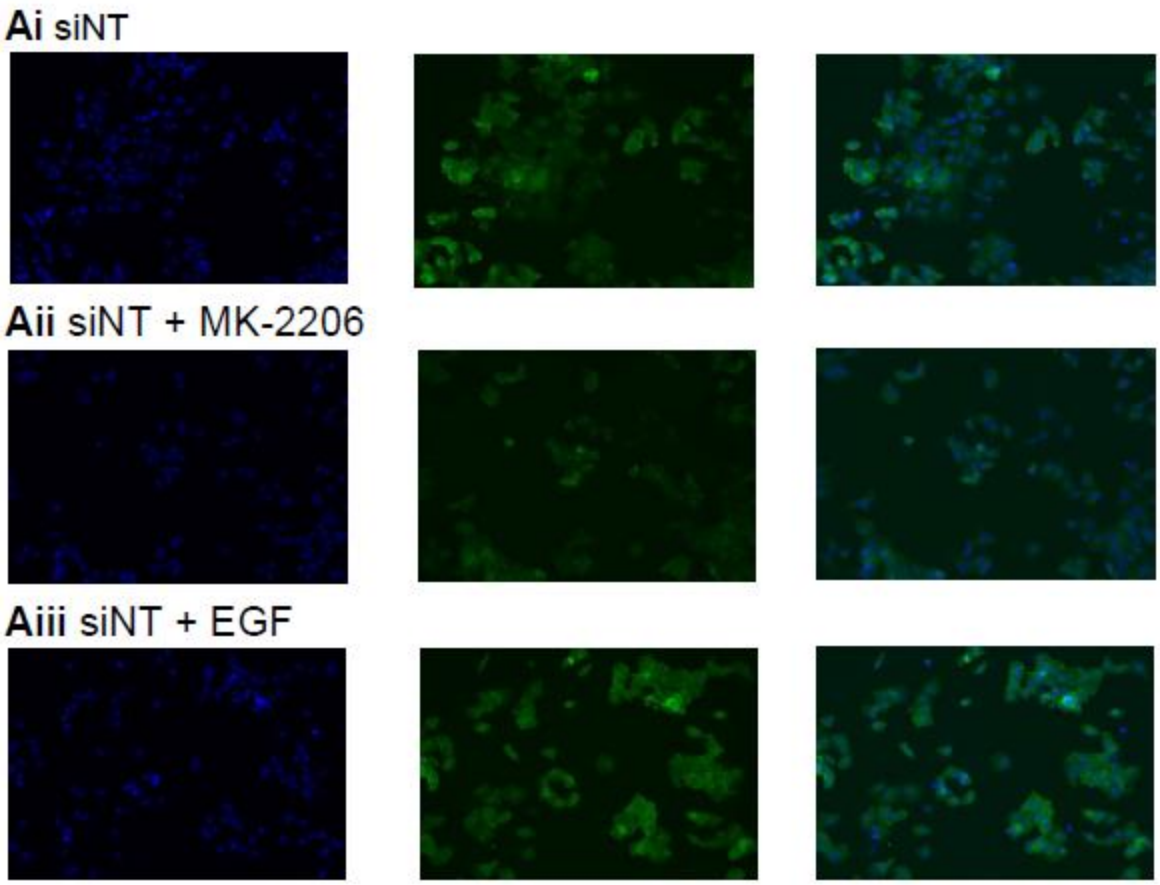

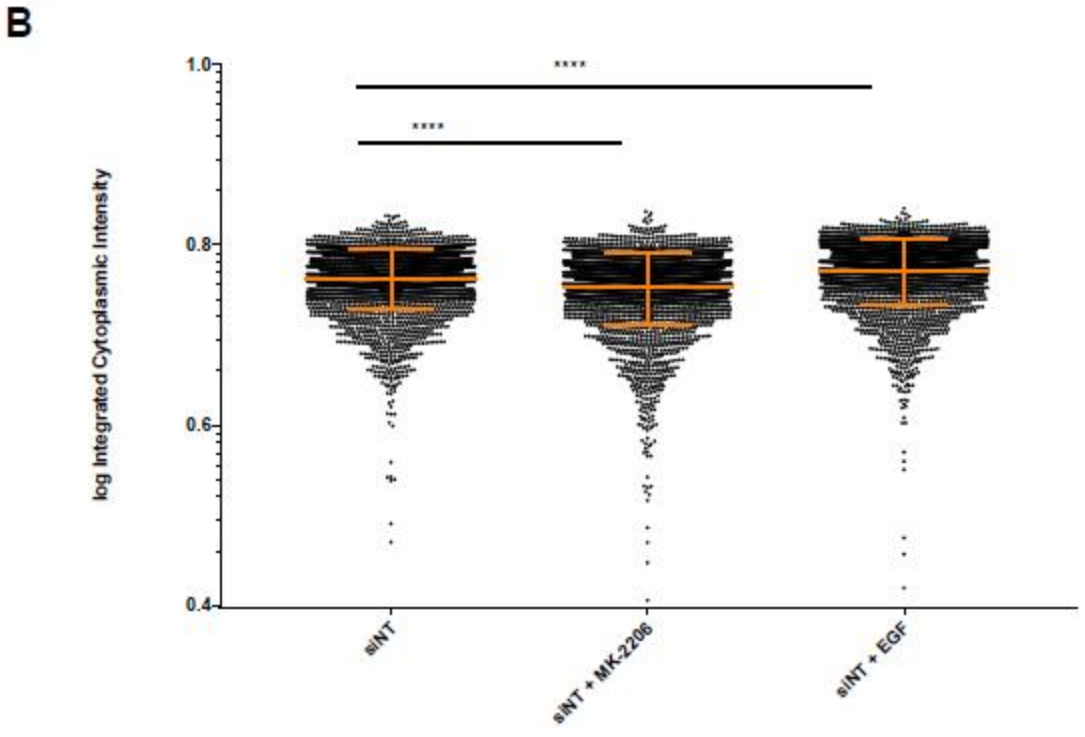

Fig. 1

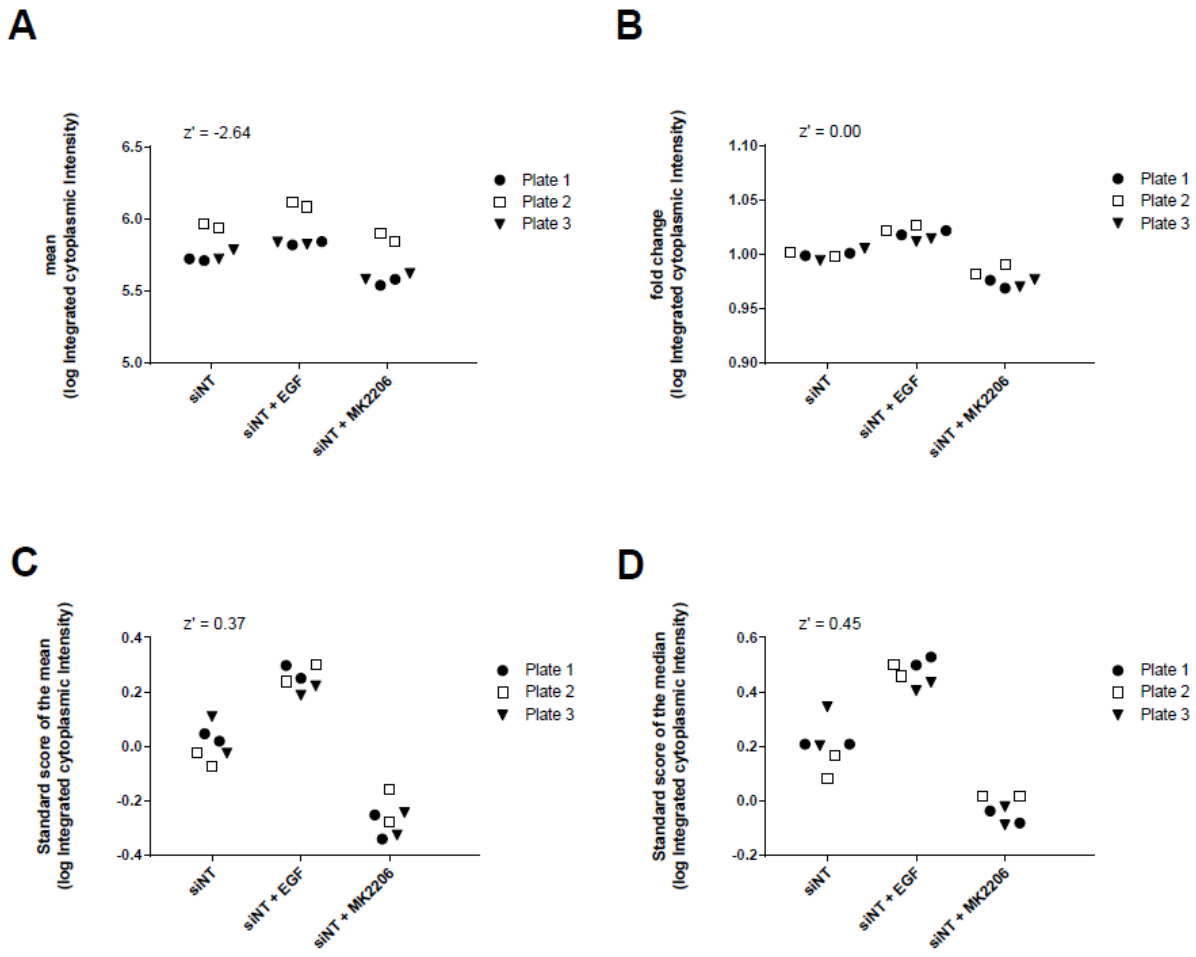

Fig. 2

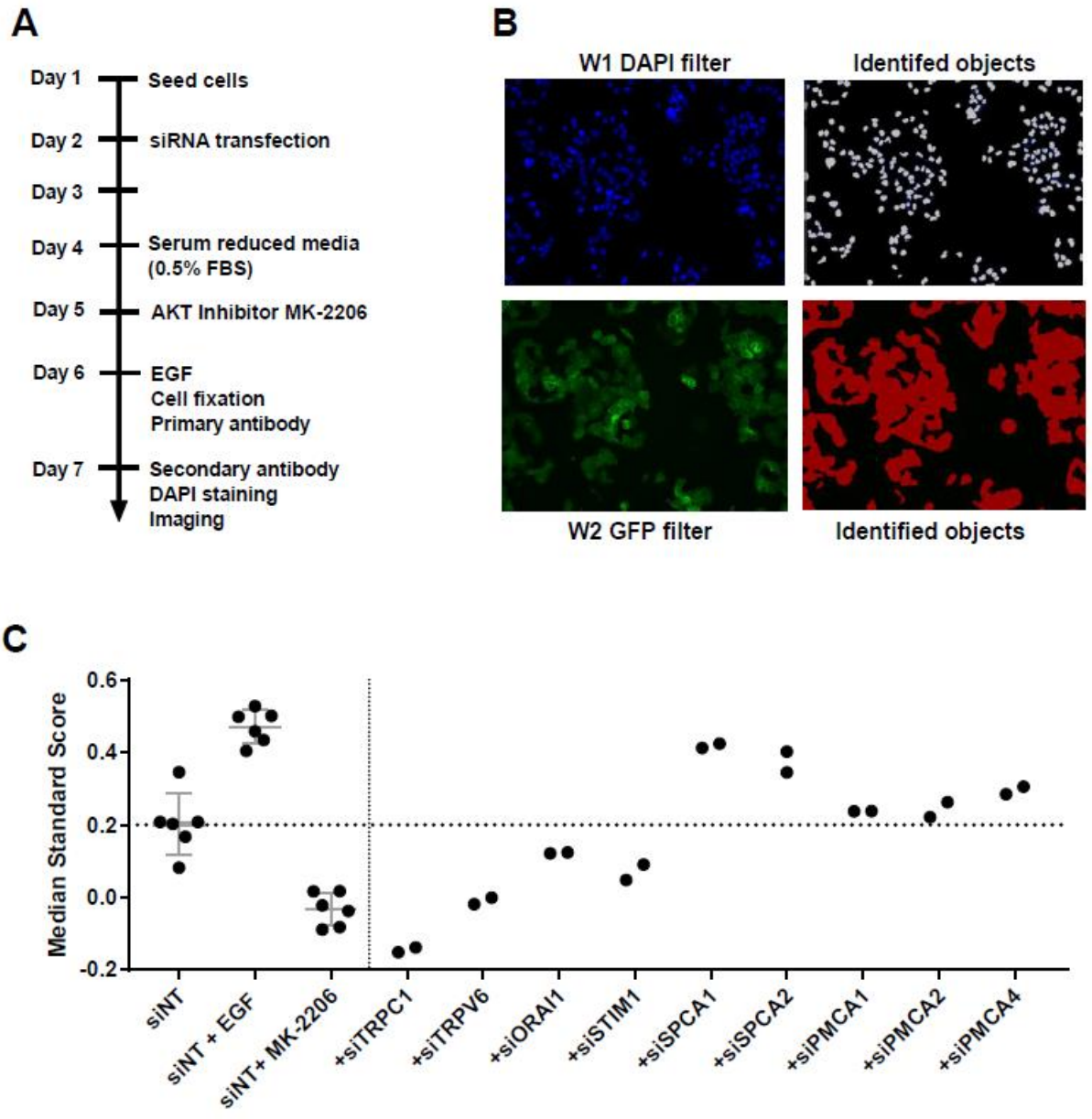

Fig. 3

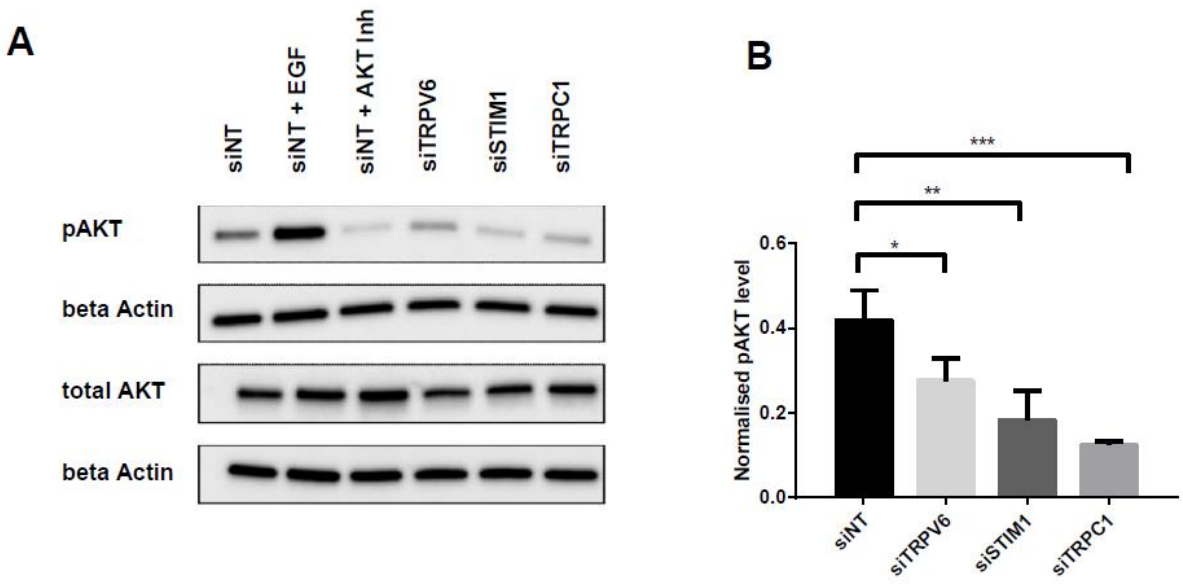

Fig. 4